Effect of the Doping Method on the Sintering Characteristics of Gadolinium-Doped Ceria

Patrizia Mangifesta, Alessandra Sanson, Edoardo Roncari
CNR-ISTEC, Faenza (RA) / Italy
Tel: +39-0546699738
patrizia.mangifesta@istec.cnr.it

Abstract

$Ce_{0.8}Gd_{0.2}O_{2-\delta}$ (GDC) is considered one of the most promising electrolyte for intermediate temperature solid oxide fuel cell (IT-SOFC). The reduction of the sintering temperature is one of the most important challenge for the production of fully dense electrolyte. The sintering behaviour of a ceramic body is strongly related to the morphological characteristics of the initial powders and can be affected by the presence of a sintering aid. The latter can be added to the main phase using several methods, ball milling and precipitation being the most generally used. The paper aims to study the influence of the doping method and of the morphology of the dopant on the sintering characteristics of GDC. GDC powders with different specific surface area were doped with 3mol% CuO via ball milling and via nitrate salt and their sintering process followed by dilatometric measurements. The results indicate that the sintering is strongly dependent on the ratio between the specific surface area of pure GDC and CuO. Moreover, the morphology of the dopant greatly affects the sintering rate. Unexpectedly, ball milling was found to be the most effective doping method for CuO-doped GDC leading to a dense electrolyte at temperature as low as 900°C.

Introduction

Ceria based ceramics have obtained extensive interest in intermediate temperature solid oxide fuel cell (IT-SOFC) due to their high ionic conductivities at 500-700°C [1]. To improve these devices, it is necessary to reduce the densifying temperature of GDC to avoid high production cost and system degradation. For this reason, many effort have been addressed to enhance the sinterability of GDC using nano-sized powders and/or using transition metal oxides (TMOs) such as CuO, CoO, Li_2O [1]. Nano-powders posses high surface area and therefore an high driving force for sintering, however the same force often leads to agglomeration and as a consequence to poor packing, low green density and heterogeneous pore structure [2]. On the other hand, TMOs allow decreasing the sintering temperature due to the alteration of grain boundary mobility. Even if the exact influence of the sintering aid on the boundary mobility depends on its nature and distribution in the sample. For CoO doped GDC for example, the improved sintering can be assigned to a grain boundary film which acts as a short circuit path improving the densification [3], whereas for CuO doped GDC the increased sinterability is due to the formation of a liquid phase of CuO that increases the boundary motion [4]. Atom diffusion in a liquid phase is much faster than in a solid one therefore, diffusional transport across the film is enhanced and consequently the boundary mobility increased [5]. From this point of view the distribution of the CuO liquid film along the grain boundary of GDC plays a key role in its sintering behaviour and as consequence it becomes of great importance to study the doping process. The addition of a dopant can induce a change in the morphology of the main powder as a function of its homogeneity and distribution in the sample. The

distribution and size of the dopant greatly affects the initial stage of sintering of the main powder, as already reported for Nickel doped Tungsten [6] and Co-doped GDC [3].
Among the possible GDC dopants, CuO is one of the more active and it less toxic and economic in respect to the more used CoO [7]. Moreover, the influence of the CuO on the sintering characteristics of GDC is important not only for its function as sintering aid. CuO-based cermets have recently received a lot of attention as catalyst for CO oxidation [8] and as substitutes of Ni cermet as anode in SOFC [9]. It is therefore important to well understand the role of this oxide on the sintering behaviour of GDC.
The most widely used doping methods are ball milling and precipitation of nitrate salt. The former provide an optimal contact between the powder particles while the second assure an high dispersion of dopant on the host powder [10]. In the present paper the sintering behaviours of pure and the CuO doped GDC were studied in relation to the powder morphology of the dopant and host powder and to the doping method. Unexpectedly the results showed that ball milling is the most suitable doping method to improve the sinterability of GDC with CuO.

Experimental

Three commercial gadolinium doped ceria, A (Praxair, UK), B (Fuel Cell Materials, USA) and C (Praxair, UK), of different specific surface area (SSA) and particle size were used as starting materials (Table 1). CuO dopant (3 mol%) was added to GDC powders as micrometric or nanometric CuO powder (Aldrich, Germany) or as copper nitrate $Cu(NO_3)_2$ solution (Fluka, Germany). In the conventional ball milling GDC and CuO powders were ultrasonically dispersed in methylethylketone (MEK) (Carlo Erba, Italy), ball-milled for 24 h in PET jar with zirconia beans and oven-dried at 100°C. The GDC+3CuO powders were grounded in agate mortar and sieved at 125 mesh.
The powder C was doped using a $Cu(NO_3)_2$ solution following the procedure described in ref. [3].
Specific surface area (SSA) of the dry powders were measured by single point B. E. T. method (Sorpty 1750, Carlo Erba, Italy, for high SSA values; FlowSorb II 2300, Micromeritics, USA, for low SSA values).
Particle size distributions were analyzed by Dynamic Light Scattering (Zetasizer Nano S Malvern). The suspensions were prepared at 5g/L in distilled water, sonicated for 6000 s and pipetted in a polystyrene cuvette. The particle size distribution was ascertained by analysing a plot of size distribution percent versus diameter (nm).
Scanning electron microscopy (SEM) (Stereoscan 360, Leica, Cambridge, UK) coupled with an energy-dispersive X-ray spectrometer (EDS) was used to analyze the powders morphology.
The dilatometric tests were carried out on a horizontal dilatometer (DIL 402E, Netzsch, Selb, Germany) on green pellets (5 x 5 x 6 mm^3) uniaxially pressed at 200 MPa and heated to the desired temperature at 10°C/min. The green density (ρ_g) and the apparent sintered density of the pellets (ρ_s) were measured geometrically and by Archimedes method respectively.

Results and Discussion

The main characteristics of the GDC powders are summarised in Tab. I and Fig. 1. Powder A and B show a low value of SSA and a three modal particle size distribution, while the nanometric nature of C is responsible for the high SSA value and it is characterised by a bi-modal particle size distribution.
The powders morphologies are shown in Fig. 1 that report a detail of the fine fraction of each powder.

Table I. Raw materials and their sintering characteristics.

Powder	SSA (m^2/g)	ρ_g (%)	T_{onset} (°C)	T_{max} (°C)	ΔL (%)	ρ_s (%)
A	5.2	55	1241	1376	10.2	92
B	9.2	56	990	1176	13.4	94
C	45.0	45	680	952	23.8	94

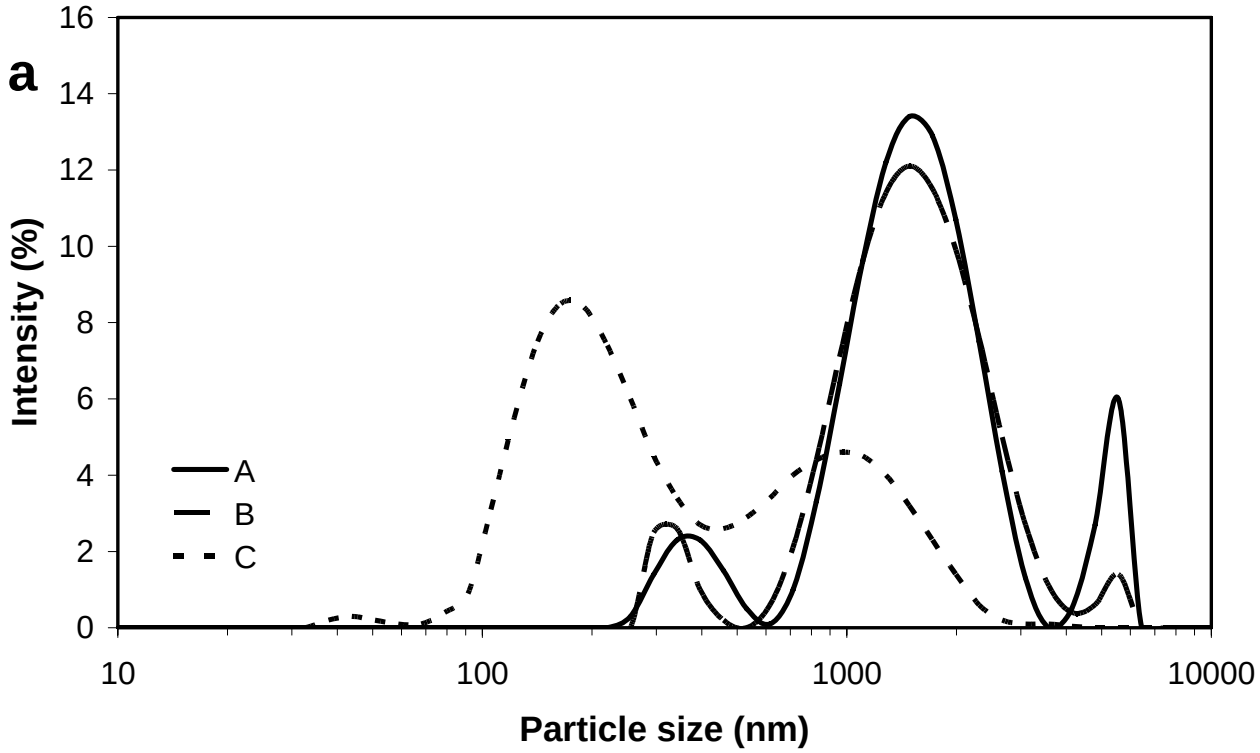

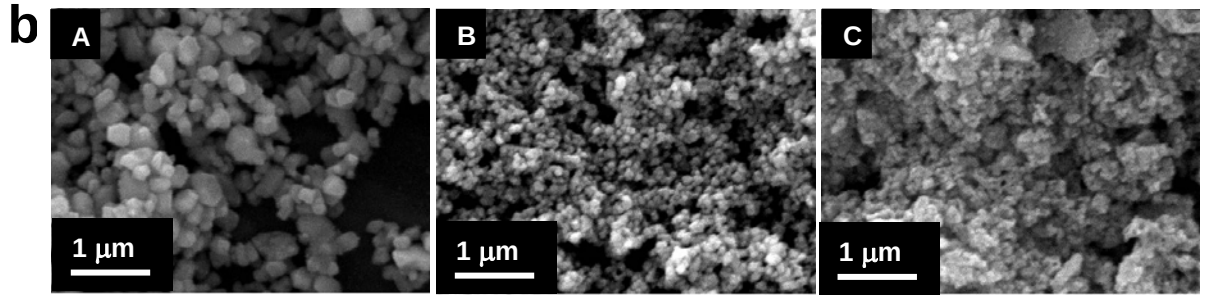

Figure 1. Morphology of the raw materials A, B and C. a) Particle size distribution, b) SEM micrograph.

The dilatometry tests done on GDC powders at constant heating rate (10°C/min) up to 1500°C are reported in Fig. 2. The shrinkage curves reflect the morphology of the powders: the high reactivity of the nanometric powder C shift toward lower values the temperature of the onset of sintering (T_{onset}) and the temperature at which the rate of shrinkage is maximum (T_{max}) (Fig. 2 and Tab. I). Generally speaking, narrower is the particle size distribution narrower will be the range of sintering ΔT ($\Delta T = T_{onset}-T_{end}$), whereas the sintering rate is inversely proportional to the particles dimension [11]. However, the informations deducted from the powder morphology are not enough to fully interpret its shrinkage behaviour. For doing so, an accurate description of the green body

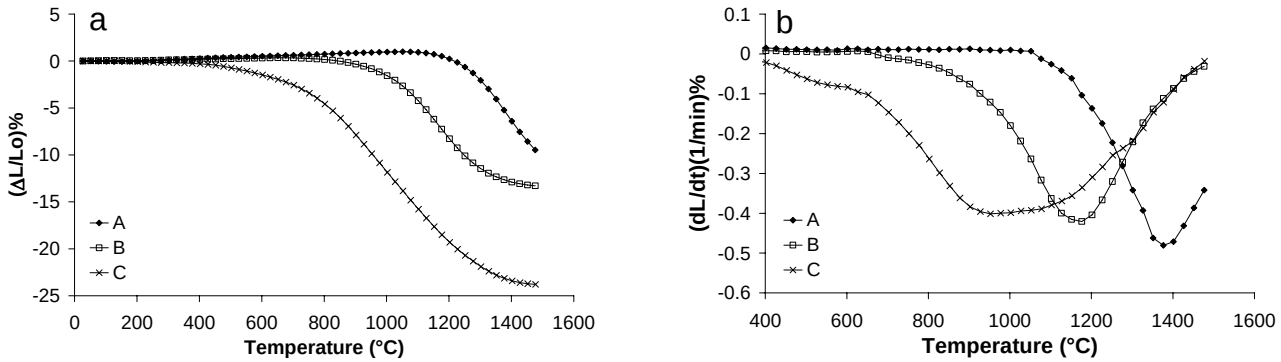

Figure 2. Sintering curves of A, B e C powders: a) linear shrinkage, b) shrinkage rate.

microstructure is necessary. For example even if C has the finest powder with very reactive fine particle, it shows the highest value of ΔT and the lowest shrinkage rate (Fig. 2). Either ΔT and the rate of shrinkage are related to the low green density (ρ_g) of C compared to the other systems (Tab. I). It has been show that the shrinkage rate decreases by a larger amount if large pores or wider pore size distribution are present [12]. The correlation between pore distribution and sintering rate can be clearly seen comparing the characteristics of A and B. Although the two systems show comparable green densities their shrinkage rates are different. This difference can be linked to the different distribution and/or dimension of the porosity in the green bodies obtained with the two powders as a consequence of a slightly different particle size distribution [13]. Therefore the shrinkage behaviour of C can be connect to the pore size and distribution in this green body. Although B and C show an almost complete sintering process, none of the sintered sample reach final relative density (ρ_s) higher than 94% (Tab. I). Other than a unfavourable powder packing this effect can be due to the reduction of Ce^{4+} to Ce^{3+} at high temperature that leads to the formation of oxygen vacancy and reduces the density as already seen for Nd-doped CeO_2 [14].

The experiments done on the pure GDC confirm the possibility to lower the sintering temperatures modifying the powders morphology. Nevertheless even with nanometric powder it is not possible to have a dense ceramic at low temperatures. To overcome this problem small amount (1-5mol%) of transition metal oxides (TMO) can be added to improve the shrinkage rate and lower the sintering temperature of GDC [1]. For this reason 3mol% CuO was added to the previous systems. This amount was chosen among 1-5mol% CuO as a consequence of sintering studies conducted in this laboratory. The results will be presented elsewhere.

As previously seen, the sinterability of a ceramic powder depend both on the starting powder morphology and the structure of the green body. In this respect it might depend on the initial state of the CuO (i. e. its initial location and size) and on the method adopted to add it to GDC. To explore this assumption the A, B and C powders were doped by ball milling with CuO of two different SSA (CuO, SSA = 1,1 m^2/g; CuO nano, SSA=24,7 m^2/g ;) and the sintering results compared with the previous ones.

The addition of micrometric CuO modifies the morphology of the starting powders inducing a slight aggregation and consequently lower value of SSA (Tab. II). This effect is clearly shown in the particle distribution of Fig. 3 where the peak relative of the finer particle disappeared. For C the aggregation affects also the larger particles shifting the average particle dimension towards higher values (Fig. 1 and 3). This effect leads to a general decrease in ρ_g as a consequence to less favourable particle packing. The comparison between the sintering behaviour of pure and doped powders is presented in Fig. 4. For each doped sample the sintering ends at a temperature well below the value typical for the pure one.

Table II. Doped powders containing 3mol% CuO and their sintering characteristics.

Powder	SSA (m^2/g)	ρ_g (%)	T_{onset} (°C)	T_{max} (°C)	ΔL (%)	ρ_s (%)
A+3CuO	5.0	52	921	950	15.3	97
B+3CuO	8.6	55	850	935	16.9	95
C+3CuO	33.6	39	873	920	25.6	94

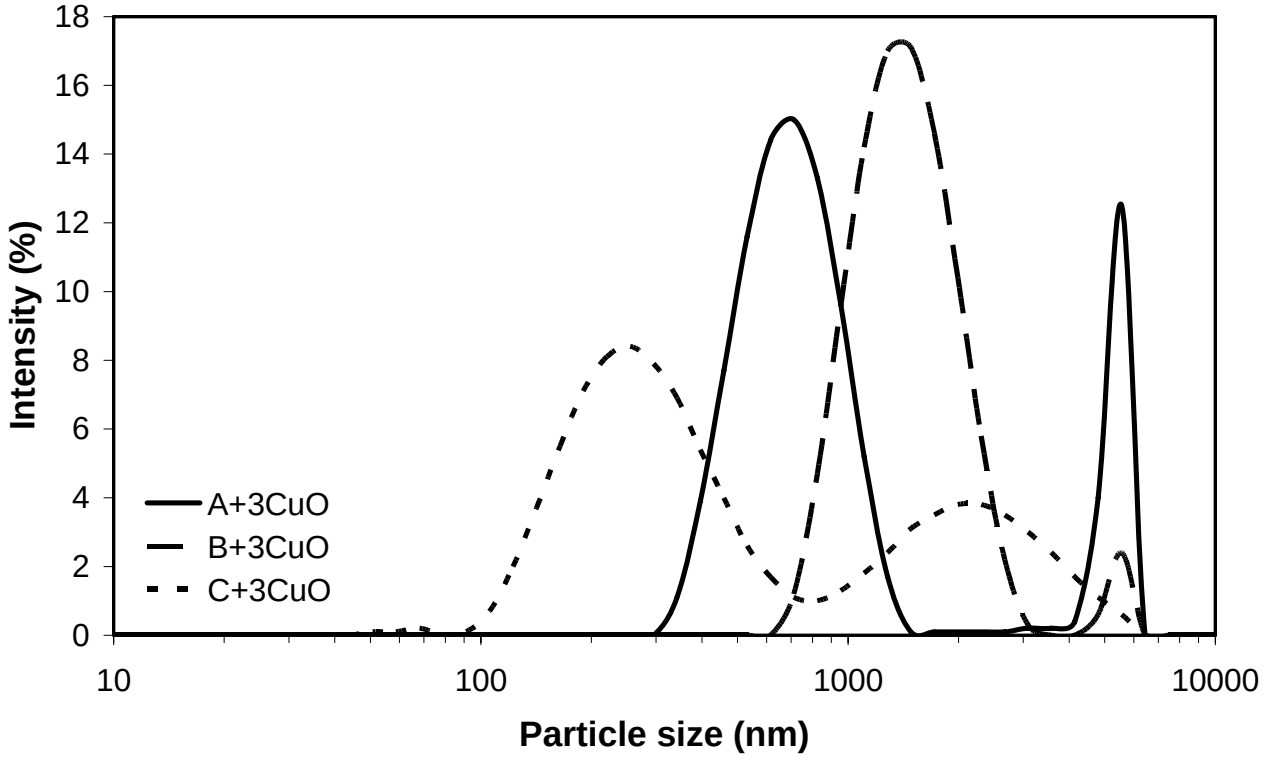

Figure 3. Particle size distribution of GDC doped powders: A+3CuO, B+3CuO and C+3CuO.

powders. This effect is due to a liquid phase induced by CuO that reduces the interparticles friction easing the rearrangement of the particles during sintering [4]. The lower temperature allow to note two maxima in the sintering rate curve of A+3CuO. This trend can be correlated to the bimodal particle size distribution shown in Fig 3. In this situation the sintering proceeds in two stages: first the fine particles and afterwards the aggregates of bigger dimensions [15]. For B+3CuO the effect is less pronounced due to the narrower particle size distribution while the high reactivity of the C+3CuO leads to a single peak. The sintering rate doubled passing from A and B to A+3CuO and B+3CuO and increases of almost 8 times for C+3CuO. This improvement is a consequence of the enhanced diffusion in the liquid phase formed by CuO compared with the one through the grain boundary typical of GDC [3]. The strong effect on C is linked to the higher porosity of its green body. In the viscous flow densifications the liquid phase enters in the pores increasing the contact zone between the particle grains and consequently improving the densification [16]. This flow continues as long as the porosity is high enough and sufficiently large pores exist. The high porosity of C+3CuO green body favoured the liquid phase mobility and as a consequence the shrinkage rate. Another important aspect is the influence of CuO on the T_{onset} of the three powders. For the micrometric ones (A+3CuO and B+3CuO) the T_{onset} is lower than for the pure GDC whereas C+3CuO show an higher T_{onset} than C. This later effect has been already observed by Jud et al. for Co-doped GDC. It is plausible this phenomenon to be linked to the ratio Φ_{GDC}/Φ_{CuO} ($diameter_{GDC}/diameter_{CuO}$).

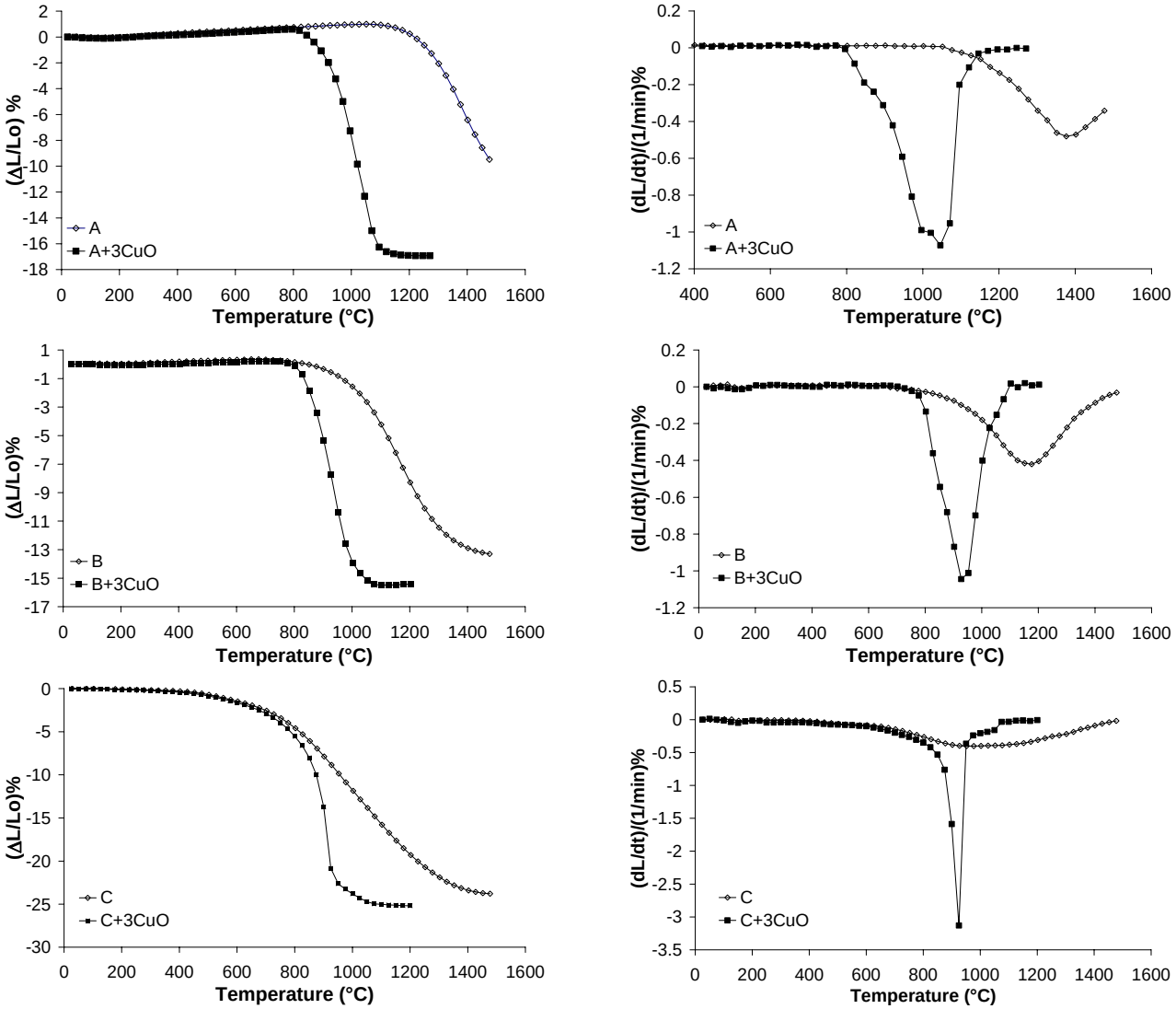

Figure 4. Sintering curves of the undoped and doped powders.

Assuming the particles to be spherical, it is possible to obtain an approximate value of their diameter Φ through the following relation(3):

$$\Phi = 6/(\rho \cdot SSA)$$

where ρ is the powder density and SSA the specific surface area The graph reported in Fig. 5 show the linearity of the relation between diameters ratio and the ΔT_{onset} (ΔT_{onset} = $T_{onsetGDC\ pure} - T_{onsetGDC\ doped}$). From this relation, when $\Phi_{GDC}/\Phi_{CuO} < 0.08$ the doped powders undergoes a lowering in T_{onset} whereas when this ratio is > 0.08 the addiction of CuO will induce an increase in the values of T_{onset}. Therefore the efficiency of a dopant in lowering the temperature of onset is higher if smaller is the ratio between the main oxide and dopant diameter. This lowering reaches a minimum related to the particle packing density and the neck space available for the dopants. Further studies are ongoing to evaluate the exact range of validity of this relation. To better understand the role played by the dimension of the dopants on the sinterability of GDC, A and C were doped with 3mol% of nanometric CuO (SSA = 24.7 m^2/g). The sintering behaviour of the powders obtained (A+3CuOnano and C+3CuOnano) is reported in Tab. III and Fig. 6. Compared to the samples doped with CuO micrometric, the addiction of CuO nano shifts for both the systems towards lower values, but if for A+3CuOnano this shift is only of few degrees, for

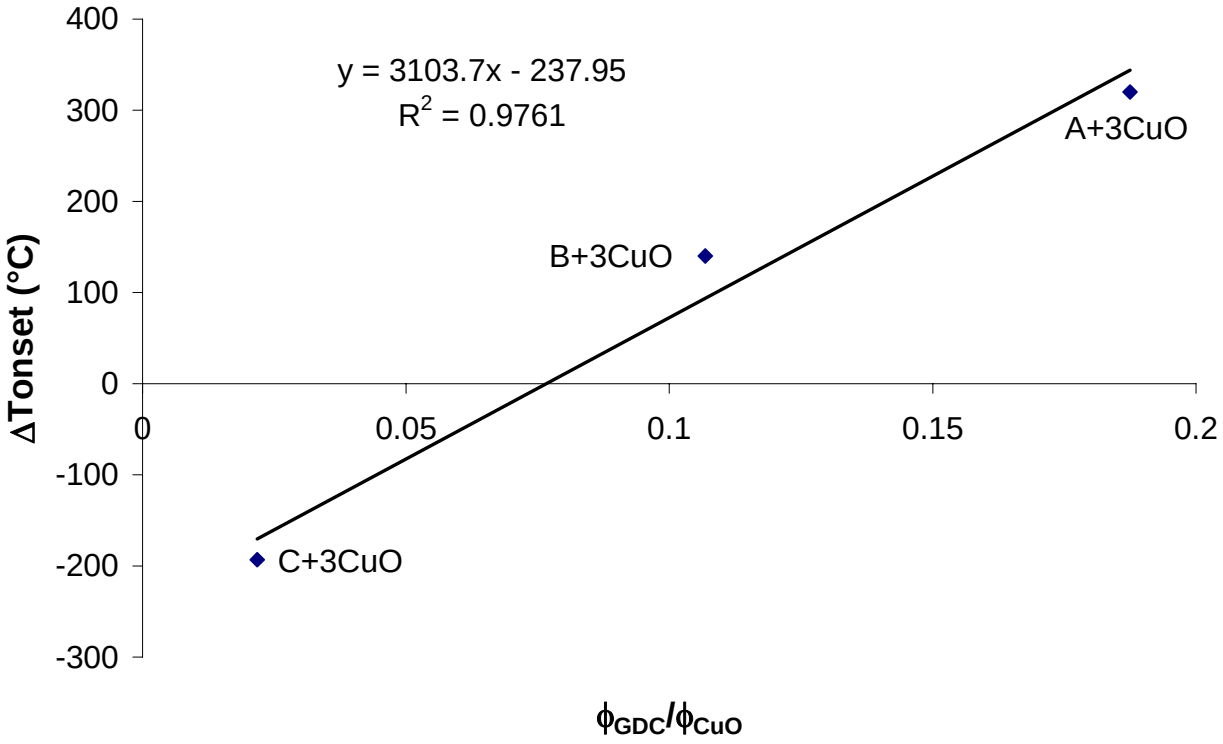

Figure 5. Plot of ϕ_{GDC}/ϕ_{CuO} as a function of ΔT_{onset}.

C+3CuOnano it reaches 83°C. It is well known that in liquid phase sintering the dopant is preferably located near the necks formed by the particles of the main phase [6]. For A the neck area can be effectively suturated already by the micrometric CuO, for this reason the introduction of a smaller dopants does not induce an huge shift. Conversely, for C only the nanometric CuO can adequately cover the necks space between the very fine particles and efficiently lowers the interparticles friction. A similar effect has been already observed in the sintering of W doped with Ni of different particle size [6]. The higher green density of C+3CuOnano compared with the one of C+3CuO is responsible for the lower shrinkage rate of the former as already noticed previously.

The dependence of the sinterability of GDC by particle size and location of the dopant, implies a possible strong relation with the doping method. For this reason C has been doped by precipitation with 3mol% of $Cu(NO_3)_2$. The doping via precipitation induces only a slight aggregation of the starting powders reflected in a lower value of SSA (Tab. IV). The sintering behaviours of C pure and differently doped are reported in Fig. 7. The samples reach the same value of linear shrinkage but different values of T_{onset} and T_{max}. As a contrary of what noted by Jud et al. [3] for Co doped GDC, ball milling with nanometric CuO seems to be the most effective combination for improving the sintering behaviour of GDC. This discrepancy can be linked to the different sintering mechanism induce by the two dopants. While Cu leads to a liquid-phase sintering mostly active at the particles necks, Co promotes the densification through the formation of a film covering the grain boundaries. The two dopants have therefore two different locations where they are mostly active. The two locations are exactly the ones induced by the different doping methods. In fact, while in the ball milling process CuO is preferentially located at the necks between the GDC particles, via precipitation the copper is added as $Cu(NO_3)_2$ that after thermal treatment covers the GDC powders with a thin film of CuO [10]. Therefore ball milling results the most effective method to dope GDC powders with CuO because the dopant directly reaches the sites where it is mostly active i. e. at the particle neck. Further

Table III. SSA and T_{onset} of A and C powders doped with two different CuO.

Powder	SSA (m^2/g)	ρ_g (%)	T_{onset} (°C)
A+3CuO	5.0	52	919
A+3CuOnano	5.2	53	913
C+3CuO	33.8	39	873
C+3CuOnano	36.3	41	790

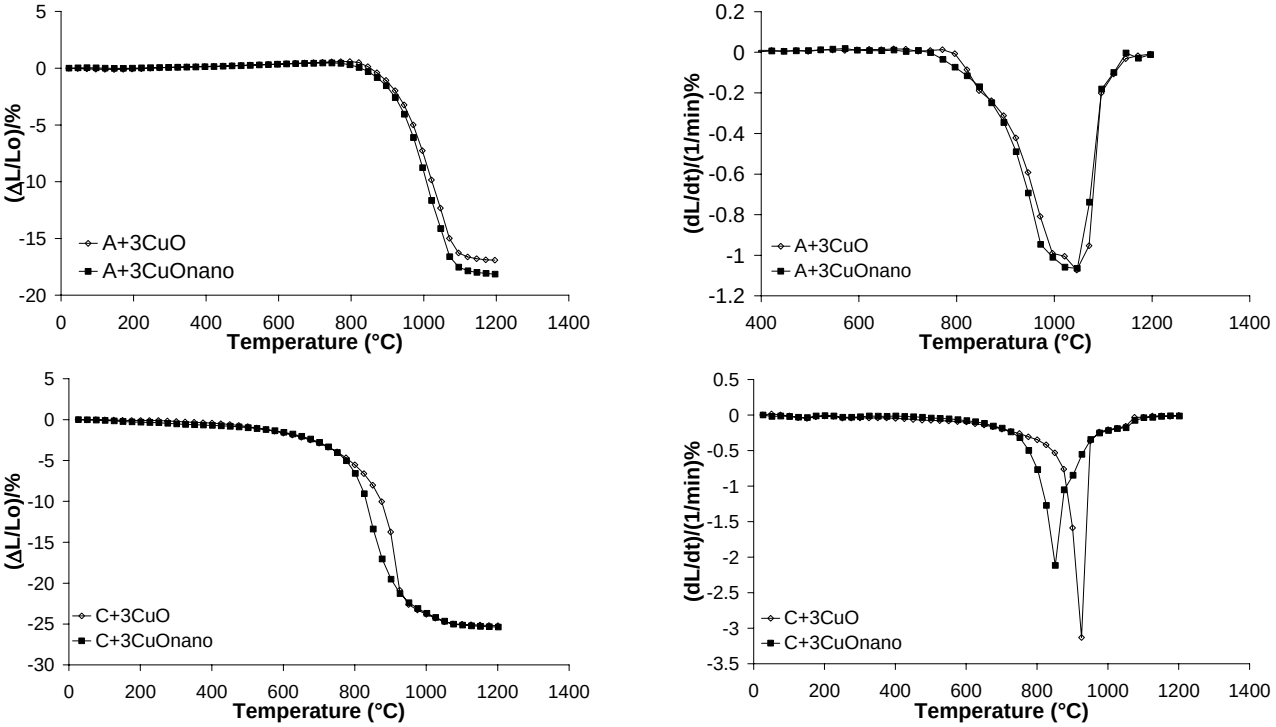

Figure 6. Sintering curves of the A and B powders doped with two different CuO.

Table IV. Pure and doped C powders, sintering characteristics.

Powder	SSA m^2/g	ρ_g (%)	T_{onset} (°C)	T_{max} (°C)
C	45.0	45	680	952
C+3CuO	33.6	39	873	920
C+3CuOnano	36.3	41	790	852
C+3CuOnit	42.8	40	849	905

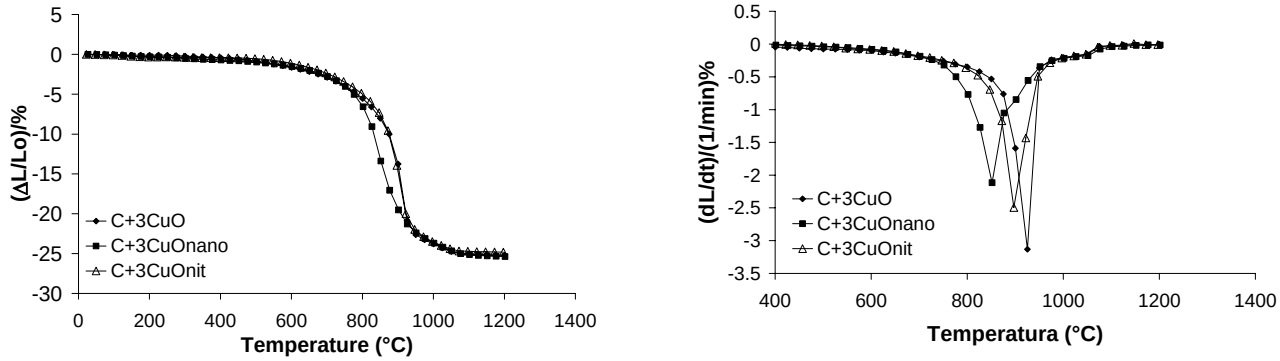

Figure 7. Sintering curves of doped C powder: C+3CuO, C+3CuOnano and C+3CuOnit.

studies are on-going to evaluate the relationship between the powder packing and the most affective dopant dimension.

Conclusions

The sintering behaviour of three commercial GDC powders of different SSA doped with 3mol% CuO of different diameter was considered. A linear relation between ΔT_{onset} and ϕ_{GDC}/ϕ_{CuO} was found. In a liquid phase sintering, the dopant is more efficient the more is able to saturate the neck space between the particles of the main phase. As a consequence, ball milling is the most effective doping method for CuO-doped GDC.

Acknowledgments

This work was funded by the Ministry of University and Research (MUR) of Italy, under the frame of the FISR Project: “Celle a combustibile ad elettroliti polimerici e ceramici: dimostrazione di sistemi e sviluppo di nuovi materiali”.

References

[1] J. D. Nicholas, L. C. De Jonghe, Prediction and Evaluation of Sintering Aids for Cerium Gadolinium Oxide. Solid State Ionics, 2007, **178**, 1187-1194.

[2] P. Bowen, T. Ziebelen, M. Staiger, H. Hofmann, C. Carry, F. Herbst, C. Legros, Slip Casting and Sintering of Ti-doped Nanosized Alumina. Key Engineering Mat., 2002, **206 - 213**, 261-264.

[3] E. Jud, L. J. Gauckler, Sintering Behavior of Cobalt Oxide doped Ceria Powders of Different Particle Sizes. J. Electroceram., 2005, **14**, 247-253.

[4] P. Mangifesta, A. Sanson, E. Roncari, Sintering Mechanism of Cuo-doped $Ce_{0.8}Gd_{0.2}O_2$ Ceramics. ECS Trans., 2007, **7** (1), 2269-2276.

[5] E. Jud, C. B. Huwiler, L. J. Gauckler, Grain Growth of Micron-sized Grains in undoped and Cobalt Oxide doped Ceria Solid Solutions. J. Ceram. Soc. Japan, 2006, **114** (11), 963-969.

[6] I. H. Moon, J. S. Kim, Y. L. Kim, The Effect of the Doping Method on the Sinterability of Nickel-Doped Tungsten Compacts. J. Less-Common Met., 1984, **102**, 219-226.

[7] X. Zhang, C. Decès-Petit, S. Yick, M. Robertson, O. Kesler, R. Maric, D. Ghosh, A Study on Sintering Aids for $Sm_{0.2}Ce_{0.8}O_{0.19}$ Electrolyte. J. of Power Sources, 2006, **162**, 480-485.

[8] T. J. Huang, Y. C. Kung, Effect of Support Sodification on Reduction and CO Oxidation Activity of doped Ceria-Supported Copper Oxide Catalyst. Catal. Lett., 2003, **85** (1-2), 49-55.

[9] A. Lashtabeg, S. J. Skinner, Solid Oxide Fuel Cells-A Challenge for Materials Chemists?. J. Mat. Chem., 2006, **16**, 3161-3170.

[10] T. Ishihara, T. Shibayama, H. Nishiguchi, Y. Takita, Nickel-Gd-doped CeO_2 Cermet Anodo for Intermediate Temperature Operating Solid Oxide Fuel Cells Using $LaGaO_3$-based Perovskite Electrolyte. Solid State Ionics, 2000, **132**, 209-216.

[11] W. D. Kingery, H. K. Bowen, D. R. Uhlmann, Introduction to Ceramics, 2nd ed., John Wiley & Sons, New York, 1976, 448-515.

[12] R. L. Coble, Sintering Crystalline Solids. II. Experimental Test of Diffusion Models in Powder Compacts. J. App. Phys., 1961, **32** (5), 793-99.

[13] J. Ma, L. C. Lim, Effect of Particle Size Distribution Sintering of Agglomerate-Free Submicron Alumina Powder Compacts. J. Eur. Ceram. Soc., 2002, **22**, 2197-2208.

[14] T. Higuchi, S. Yamaguchi, K. Kobayashi, T. Hattori, A. Fukushima, S. Shin, T. Tsukamoto, Electronic Structure of $Ce_{1-x}Nd_xO_{2-\delta}$ Probed by Soft-X-Ray Spectroscopy. Jpn. J. App. Phys., 2004, **43** (11b), 1463-1465.

[15] E. R. Leite, M. A. L. Nobre, M. D. Ribeiro, E. Longo, J. A. Varela, The Effect of Heating Rate on the Sintering of Agglomerated $NaNbO_3$ Powders. J. Mater. Sci., 1998, **33**, 4791-4795.

[16] W. Schatt, E. Friedrich, Disclocation-Activated Sintering Processes. Sintering ’85, Plenum Press, New York, 1985, 133-141.